# Quasiperiodic forcing of coupled chaotic systems

Manish Agrawal,[1] Awadhesh Prasad,[1] and Ram Ramaswamy[2]
[1]*Department of Physics and Astrophysics, University of Delhi, Delhi 110007, India*
[2]*School of Physical Sciences, Jawaharlal Nehru University, New Delhi 110067, India*
(Received 14 July 2009; published 4 February 2010)

We study the manner in which the effect of quasiperiodic modulation is transmitted in a coupled nonlinear dynamical system. A system of Rössler oscillators is considered, one of which is subject to driving, and the dynamics of other oscillators which are, in effect, indirectly forced is observed. Strange nonchaotic dynamics is known to arise only in quasiperiodically driven systems, and thus the transmitted effect is apparent when such motion is seen in subsystems that are not directly modulated. We also find instances of imperfect phase synchronization with forcing, where the system transits from one phase synchronized state to another, with arbitrary phase slips. The stability of phase synchrony for arbitrary initial conditions with identical forcing is observed as a general property of strange nonchaotic motion.

DOI: 10.1103/PhysRevE.81.026202 PACS number(s): 05.45.Xt, 05.45.Pq

## I. INTRODUCTION

Among the diverse dynamical states encountered in the study of nonlinear dynamical systems, strange nonchaotic attractors (SNAs) that are created when there is quasiperiodic driving [1] are of particular interest. These attractors are fractal in structure, but the motion has negative or zero Lyapunov exponents. SNAs are an example of transitional dynamics, occurring between regimes of chaotic strange attractors [2] and quasiperiodic tori that are neither strange nor chaotic.

The focus in the present work is the dynamics of coupled nonlinear oscillators when one of them is subject to external quasiperiodic driving. Our interest is in understanding the manner in which the effect of such driving is transmitted via the coupling and the motivation arises from the fact that in a variety of natural systems that are subject to forcing, the modulation can be either direct, namely, when a given system is itself subject to driving or indirect when it is coupled to another system which is being externally modulated. For instance, biological phenomena exhibit stability while being intrinsically aperiodic [3]. The source of aperiodicity is not always clear, raising the possibility that such behavior may be caused by indirect modulation. Further, given the current interest in networks of coupled dynamical systems [4], this question is of particular importance.

Coupled nonlinear dynamical systems, even in the absence of external driving, display a range of interesting behavior that includes synchronization, hysteresis, and phase locking [5,6]. While synchronization in its various forms is common in coupled nonlinear systems [5–11], the phase synchronization induced by external driving has not been studied in detail. This is important in view of potential applications to disciplines ranging from physics, chemistry, and biology to medical sciences [12].

In this paper we examine the dynamics of modulated coupled oscillator systems and analyze the dynamics of the *indirectly* forced subsystem. The model system and our numerical studies are discussed in Sec. II, where we also present the different dynamical behaviors that are possible. Although the present study focuses on Rössler oscillators, similar results can be obtained in other driven dissipative dynamical systems as well. In Sec. III we discuss phase synchronization and the effects of quasiperiodic forcing. It is observed that when the strength of forcing is increased, long temporal segment of perfect phase synchrony is replaced by short synchronous segments separated by phase slips. In Sec. IV we analyze the dynamics on strange nonchaotic attractors for phase synchrony in a network of oscillators. The paper concludes with a summary in Sec. V.

## II. DYNAMICAL REGIMES

We consider two symmetrically and diffusively coupled Rössler oscillators (distinguished by subscripts 1 and 2)

$$
\begin{aligned}
\dot{x}_1 &= -\omega_1 y_1 - z_1 + \epsilon(x_2 - x_1),\\
\dot{y}_1 &= \omega_1 x_1 + a y_1[1 + f(\cos t + \cos \Omega t)],\\
\dot{z}_1 &= b + z_1(x_1 - c),\\
\dot{x}_2 &= -\omega_2 y_2 - z_2 + \epsilon(x_1 - x_2),\\
\dot{y}_2 &= \omega_2 x_2 + a y_2,\\
\dot{z}_2 &= b + z_2(x_2 - c),
\end{aligned}
\qquad (1)
$$

with one (system 1) being subject to quasiperiodic forcing. The coupling constant is $\epsilon$, and the system parameters taken are $a=0.06$, $b=0.1$, and $c=14.0$. The frequencies $\omega_1=0.99$ and $\omega_2=0.95$ are mismatched, making the interacting subsystems nonidentical. Modulation occurs through the term $f(\cos t+\cos \Omega t)$, where $f$ is the amplitude and $\Omega=(\sqrt{5}-1)/2$ is the irrational frequency that makes the drive quasiperiodic in time. The setup is depicted in Fig. 1.

Shown in Fig. 2 is a schematic phase diagram of the dynamical regimes as a function of the parameters $f$ and $\epsilon$. The separating curves of different regimes are based on numerics (see Fig. 2 caption). The regions marked 1-T and 2-T denote single- and double-band quasiperiodic tori respectively,

 

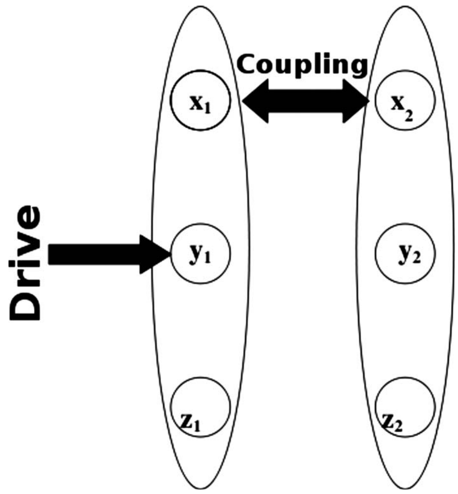


FIG. 1. Coupling scheme in the present model. The two oscillators are symmetrically and bidirectionally coupled through one of the variables, here $x$, while one of the oscillators is subject to quasiperiodic driving through a different variable, here $y$.

while C1 and C2 correspond to the different regions of chaotic dynamics. SNAs are found in the shaded regions; the symbols TC, GF1, GF2, and I indicate that these are formed by different "routes," namely, torus collision [13], fractalization [14], and intermittency [15,16]. These routes (strange to nonstrange attractors) can be deduced via visual examination of the Poincaré sections (see Fig. 4—identification details are reported in Ref. [1]). The labels 1 and 2 indicate that the SNAs or chaotic attractors in different regions have differing morphologies.

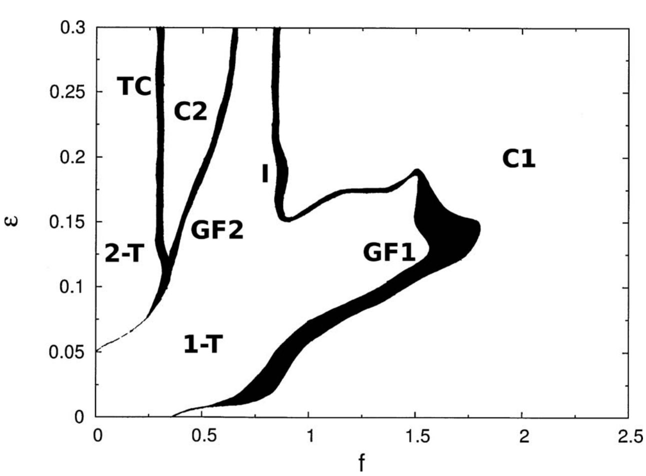


FIG. 2. Phase diagram (schematic) for the coupled Rössler system, Eq. (1) as a function of $f$ and $\epsilon$. Double band and single band quasiperiodic torus regions are marked 2-T and 1-T, respectively, while C1 and C2 correspond to chaotic dynamics. SNAs occur in the shaded regions TC, GF1 and GF2, and I denoting the different routes by which they are formed as discussed in the text. This figure is generated by calculating the Lyapunov exponents by taking a grid of $100\times 100$ points in the parameter space. The boundaries of chaotic regimes are determined from the $\lambda=0$ contour while nonstrange to strange regimes are deduced via examination of Poincaré sections—see the text for details.

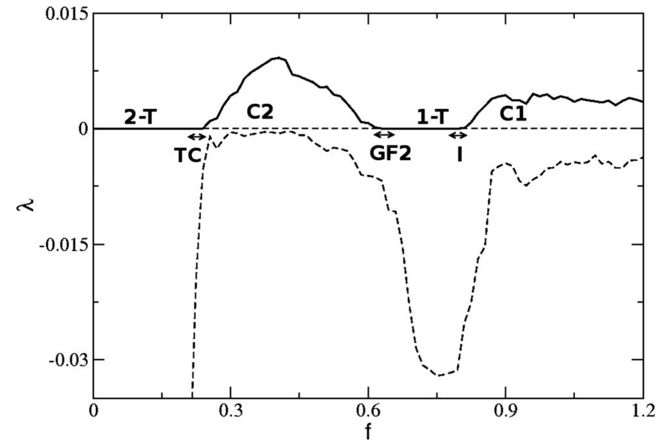


FIG. 3. The two largest nonzero Lyapunov exponents as a function of forcing amplitude $f$ for $\epsilon=0.25$. This selected range of forcing strength contains all the dynamical states as shown in Fig. 2.

The dynamical states and the transitions between them can be identified by examination of the spectrum of Lyapunov exponents. The present system has a total of six exponents, the largest two of which are shown as a function of $f$ for fixed $\epsilon$ in Fig. 3.

We examine the dynamics of the oscillator that is indirectly forced, namely, subsystem 2. Poincaré sections in the $[y_2, \psi=\mathrm{mod}(t,2\pi)]$ plane are shown in Fig. 4 in different regions of parameter space. The leftmost panel shows the creation of SNAs due to torus collision, namely, the two-band quasiperiodic tori colliding with its unstable parent to form a single-band attractor when the parameter $f$ is increased. The middle panels show the fractalization (GF) route to the occurrence of SNAs. In this *fractalization* route

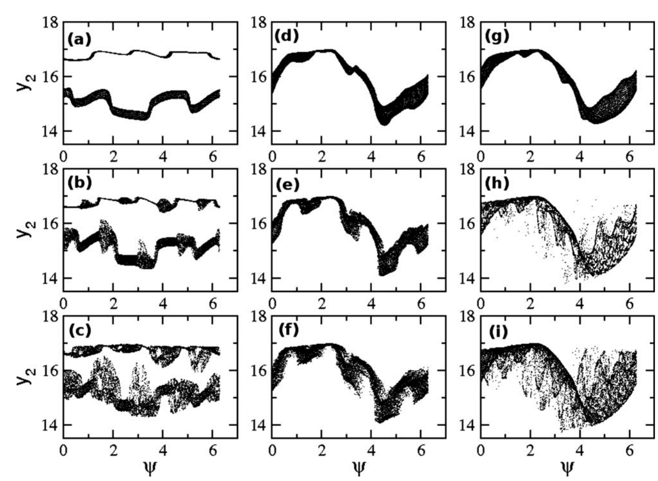


FIG. 4. Poincaré sections for the indirectly forced subsystem, showing the evolution of the dynamics, from quasiperiodic tori to chaotic attractors (CAs) through different routes to SNAs, keeping $\epsilon=0.25$. The left panel shows the torus collision TC route: (a) torus $f=0.213\,274$, (b) SNA $f=0.246\,043$, and (c) CA $f=0.270\,203$. Middle panel shows the fractalization GF route: (d) torus $f=0.680\,644$, (e) SNA $f=0.627\,326$, (f) CA $f=0.604\,277$. Right panel shows the intermittency I route: (g) torus $f=0.760\,622$, (h) SNA $f=0.809\,220$, (i) CA $f=0.822\,827$. The Poincaré sections are taken at $x_2=0$, and $\psi=\mathrm{mod}(t,2\pi)$.

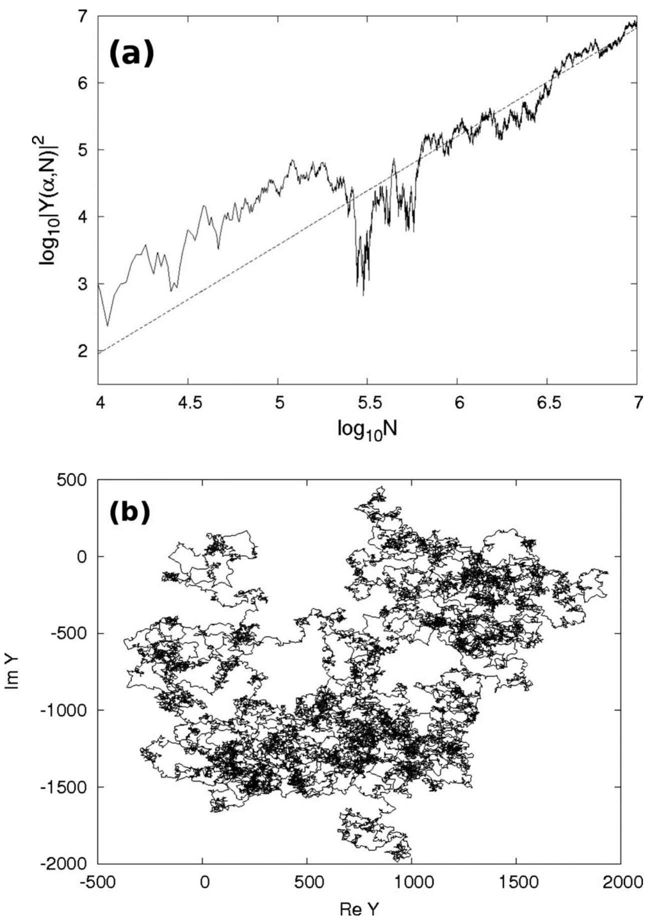


FIG. 5. Singular-continuous spectrum analysis of the $\{(y_2)_k\}$ time series at $\epsilon=0.25$ and $f=0.627\,326$, namely, panel (e) in Fig. 4. (a) Plot of $Y(\alpha,N)$ vs $N$ showing the power-law scaling; the slope is $\approx 1.63$. (b) The fractal path in the complex plane $(\mathrm{Re}[Y],\mathrm{Im}[Y])$.

for the creation of SNAs a quasiperiodic torus get increasingly wrinkled with the change in forcing amplitude, and becomes a strange set before becoming the chaotic attractor. The right panel depicts the intermittency scenario [15].

In order to quantitatively confirm that the dynamics in subsystem 2 is strange and nonchaotic, we use measures that have been suggested earlier [1,17,18], in particular the singular-continuous spectrum analysis [17]. We compute the Fourier transform [19,20] as

$$Y(\alpha,N)=\sum_{k=1}^{N}(y_2)_k\exp(i2\pi k\alpha), \tag{2}$$

where $\alpha$ is proportional to the irrational driving frequency $\Omega$ and $\{(y_2)_k\}$ is the time series of the variable $y_2$ of length $N$. The Fourier transform scales with $N$ as [17]

$$|Y(\alpha,N)|^2\sim N^{\mu}, \tag{3}$$

where $1<\mu<2$ is a scaling exponent. The time evolution of $Y(\alpha,N)$ can be represented by an orbit or a *walker* in the complex plane $(\mathrm{Re}[Y(\alpha,N)], \mathrm{Im}[Y(\alpha,N)])$, and for a singular-continuous spectrum (which is the case if the dynamics is strange) it implies that the walk on the plane $(\mathrm{Re}[Y],\mathrm{Im}[Y])$ will be a fractal [19].

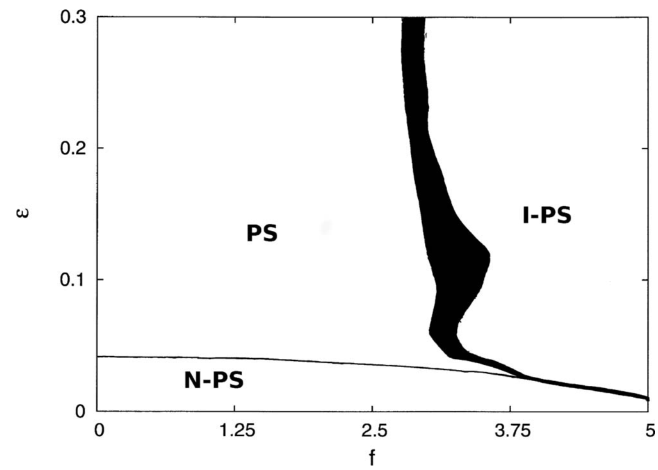


FIG. 6. The schematic phase diagram for the coupled Rössler system [Eq. (1)] in the $f$-$\epsilon$ parameter space. Here PS is the phase synchronization region, I-PS represents the Imperfect phase synchronization region, and the region where oscillators remain unsynchronized is represented by N-PS. This figure is generated by calculating the phase difference in a $100\times100$ grid.

Shown in Fig. 5(a) is a plot of $|Y(\alpha,N)|^2$ vs $N$ for $\alpha=\Omega/4$ which has the scaling exponent $\mu\approx1.63$, and the walk in Fig. 5(b) appears to be fractal, suggesting that the dynamics of the subsystem is indeed strange and nonchaotic, in consonance with the Lyapunov exponents. As has been pointed out earlier, SNAs have a locally unstable but globally stable character [1,18,21]. The distribution of finite-time Lyapunov exponents (FTLEs) can be used to further characterize SNAs: the mean of the distribution is negative, while the tail extends into the positive FTLE region (results not shown here).

## III. PHASE SYNCHRONIZATION

A number of recent studies have established that phase synchrony is an important dynamical state in coupled systems [11,22]. Here we study the phase synchronization which can be *induced* by an external quasiperiodic drive. For Rössler oscillators given by Eq. (1), the phase is defined as [23,24] $\phi_i\sim\arctan y_i/x_i$, $i=1,2$. Shown in Fig. 6 are regimes (marked PS) of phase synchronization in the parameter space, namely, when the phase difference between two oscillators $|\phi_2-\phi_1|$ does not grow in time [22] while N-PS in Fig. 6 indicates regions where the oscillators are not synchronized.

With increase in forcing amplitude, phase synchronization is obtained at lower coupling strength. This result is of potential utility in cases where direct access to the internal coupling parameter of coupled natural systems is difficult: phase synchronization can be tuned via appropriate external forcing. To further illustrate this point, the evolution of phase difference $|\phi_2-\phi_1|$ with time is shown in Fig. 7 for two different values of forcing strengths at $\epsilon=0.035$. As shown in Fig. 7 at $f=0.806\,18$ (N-PS) the phase difference remain

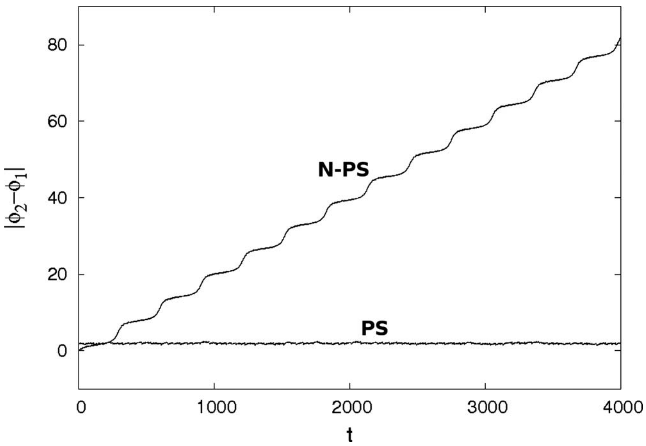


FIG. 7. Phase difference between the oscillators of coupled Rössler system with time for unsynchronous ($f$=0.806 18) and synchronous ($f$=2.815 38) states at $\epsilon$=0.035.

unbounded with time, but as the forcing is increased while keeping other parameters fixed, we observe a transition from unsynchronized state to a phase synchronous state at $f$=2.815 38 (PS).

Comparing Figs. 2 and 6 it can be seen that PS is possible in either torus, SNA or when the motion is chaotic. Similarly, when the oscillators are unsynchronized (i.e., N-PS regime in Fig. 6) the subsystem dynamics can be regular, chaotic, or strange nonchaotic as well.

In the region of imperfect phase synchrony, marked I-PS in Fig. 6 the subsystems are phase locked, subject to occasional slips. The value of $|\phi_2-\phi_1|$ varies during the evolution of the chaotic system [25], changing as in Fig. 8, in a stepwise manner. Each step corresponds to a phase synchronized (PS) state under a particular phase locking condition. The jump between two consecutive steps occurs in (arbitrary) multiples of $\pi$. This is probably a consequence of the quasiperiodic drive since in a periodically forced system [25] the phase difference is always a fixed multiples of $\pi$. The inset of Fig. 8 shows an expanded view of the phase jump.

In the transition regime from PS to I-PS there is region of coexistence of both these types of synchronization, with the basins of the two attractors being riddled (results not shown here). In contrast, in quasiperiodically driven coupled maps where several attractors coexist [26], smooth boundaries are observed.

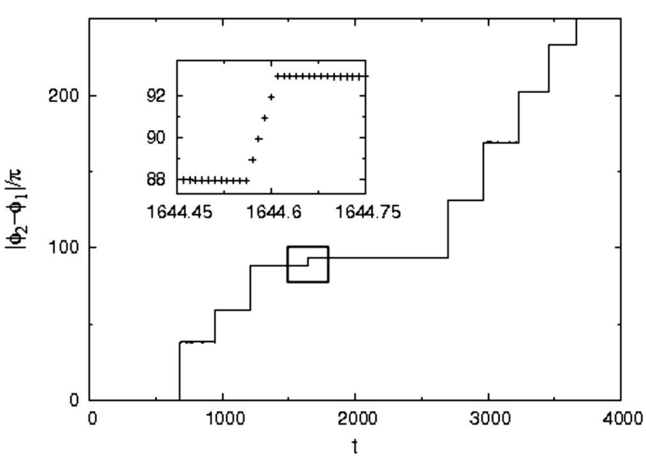


FIG. 8. Phase difference with time in imperfect phase synchronization state for $\epsilon$=0.15, and $f$=3.732 11. The inset figure shows the expanded view of the selected region for a jump.

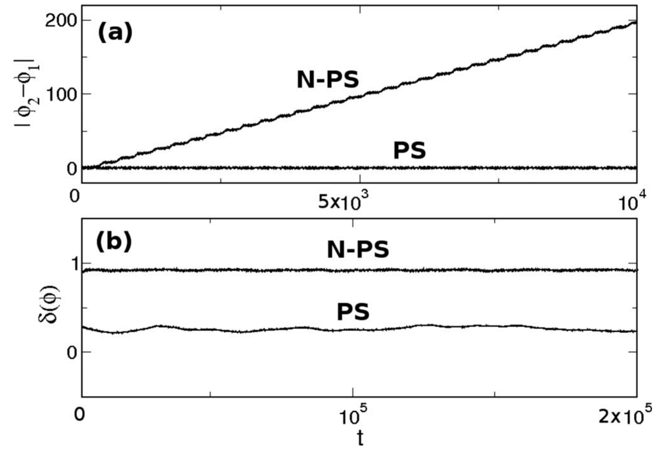


FIG. 9. Phase difference between the (a) oscillators and (b) coupled system and its copy at the same forcing, but starting at different initial conditions, for SNAs in N-PS ($\epsilon$=0.035, $f$=0.795 38) and PS ($\epsilon$=0.125, $f$=1.618 55).

## IV. SNA AND PHASE SYNCHRONY

Comparison of Figs. 2 and 6 suggests that PS or unsynchronized (N-PS) dynamics can arise independent of the nature of the dynamical state, namely, on tori, SNAs or on chaotic attractors. In order to see the difference between SNAs in PS and N-PS regimes of Fig. 6, we plot the phase differences between the oscillators starting from different initial conditions in Fig. 9(a). These curves show that the SNAs in PS regime are phase synchronized while SNAs in N-PS regime are out of phase synchrony.

An important property of SNAs is that starting from different initial conditions, trajectories of a system, and its copy subject to *identical* forcing also evolve in unison as a function of time [27]. We further examine this property of SNAs in terms of the *phase* synchronization. $\delta(\phi)$ represents the phase difference between the phase of coupled system and its copy at the same forcing, but starting at different initial conditions. Phase difference $\delta(\phi)$ is shown in Fig. 9(b) for the SNAs in the PS and N-PS regimes. The curves in Fig. 9(b) clearly show that for SNAs in both PS and N-PS regimes, the phase difference between the system and its copy remains bounded.

Similar effects are seen in a network of oscillators with nearest-neighbor diffusive coupling with periodic boundary conditions (we consider $N$=10) where one of them is subject to quasiperiodic forcing. We consider the case where the forced oscillator ($\omega_1$=0.99) is not identical to the remaining oscillators ($\omega_i$=0.95, $i$=2,3,...,10). Figures 10(a)–10(c) correspond to the torus, SNA, and chaotic attractor at $f$=2.5, 9.761 65, and 10.781 65, respectively, for coupling strength $\epsilon$=0.25. We have verified the presence of SNAs along with other dynamics for all oscillators that are coupled with the forced oscillator. Shown in Figs. 10(d) and 10(e) are

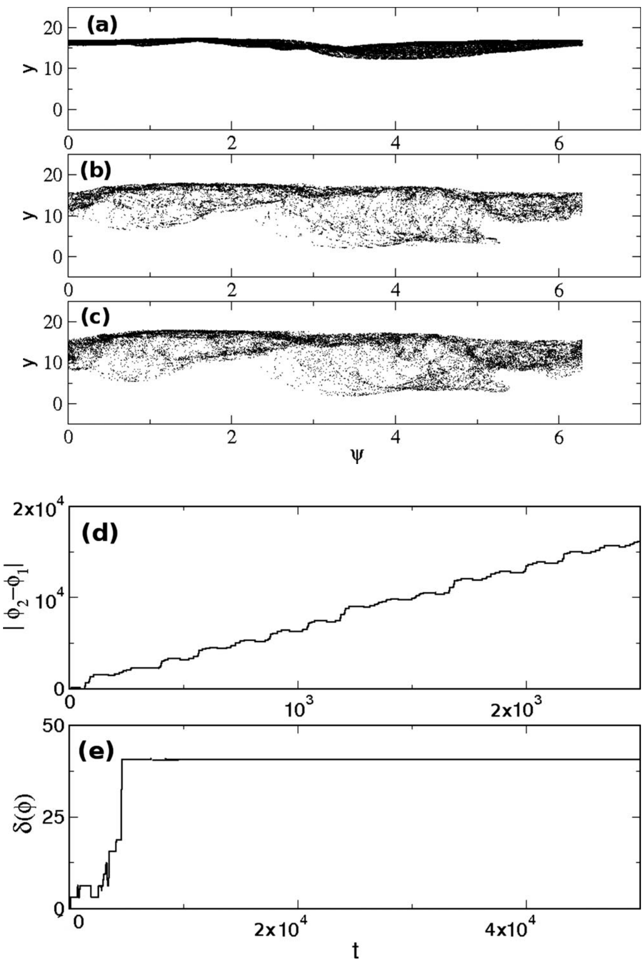


FIG. 10. Poincaré sections of (a) torus at $f=2.5$, (b) SNA at $f=9.761\,65$, and (c) chaotic attractors at $f=10.781\,65$. The phase relations (d) $|\phi_2-\phi_1|$ and (e) $\delta(\phi)$ with time for SNA.

the phase differences between nearest neighbors $|\phi_2-\phi_1|$ and the phase difference between the system and its copy $\delta(\phi)$, respectively, for the SNAs. These curves clearly confirm the above mentioned stable-phase property of SNAs [where $\delta(\phi)$ remains bounded] while the oscillators remain unsynchronized (unbounded $|\phi_2-\phi_1|$).

## V. SUMMARY

The manner in which external modulation is *transmitted* through coupling has been the subject of the present paper. By focusing on the creation of strange nonchaotic dynamics, it has been possible for us to examine the effect of driving in an unambiguous manner since it is well-known that the quasiperiodic modulation of nonlinear dynamical systems frequently leads to the formation of SNAs. Thus strange nonchaotic motion that is seen in the subsystem dynamics must arise through the quasiperiodic modulation that effectively arises via the coupling.

We have studied a system of symmetrically coupled nonlinear oscillators, with a single one of them being subjected to external quasiperiodic driving, and examine the dynamics of another of the (sub)systems. We consider the case of two oscillators in detail; results are also obtained for a larger chain of oscillators (we have also studied networks of different topologies [28]). The occurrence of strange nonchaotic dynamics can be verified, and these also appear to be formed through the different standard routes [13–16]. Identification of strange nonchaotic dynamics in indirectly forced systems can be of advantage in cases where it is not possible to directly access the subsystem of interest. Through suitable coupling, therefore, it may thus still be possible to effect stabilization and control.

Phase stability of coupled system over different initial conditions under identical forcing is established as a general property of SNAs, which occurs irrespective of the number of coupled oscillators and different synchronization states between the coupled oscillators.

We find that there are regimes of phase synchronization as well as unsynchronized states. In particular, a quasiperiodic drive can provide phase synchronization for lower coupling strengths, while the possibility of imperfect phase synchronization in coupled systems can have useful applications in, for instance, controlling human cardiorespiratory activity [29] or neuronal systems [30].

## ACKNOWLEDGMENTS

M.A. is grateful to UGC for RFSMS support, and A.P. and R.R. would like to thank the DST, Government of India for financial support.

[1] C. Grebogi, E. Ott, S. Pelikan, and J. A. Yorke, Physica D **13**, 261 (1984); A. Prasad, S. Singh Negi, and R. Ramaswamy, Int. J. Bifurcation Chaos Appl. Sci. Eng. **11**, 291 (2001); U. Feudel, S. Kuznetsov, and A. Pikovsky, *Strange Nonchaotic Attractors* (World Scientific, Singapore, 2006).

[2] D. Ruelle and F. Takens, Commun. Math. Phys. **20**, 167 (1971).

[3] J. D. Murray, *Mathematical Biology* (Springer-Verlag, New York, 1993), and the references therein.

[4] M. Barahona and L. M. Pecora, Phys. Rev. Lett. **89**, 054101 (2002); H. Hong, M. Y. Choi, and B. J. Kim, Phys. Rev. E **65**, 026139 (2002); C. Li, W. Sun, and J. Kurths, *ibid.* **76**, 046204 (2007).

[5] A. S. Pikovsky, M. G. Rosenblum, and J. Kurths, *Synchronization: A Universal Concept in Nonlinear Sciences* (Cambridge University Press, Cambridge, England, 2001).

[6] K. Kaneko, *Theory and Applications of Coupled Map Lattices* (Wiley, New York, 1993); E. Ott, *Chaos in Dynamical Systems* (Cambridge University Press, Cambridge, 1993); L. M. Pecora and T. L. Carroll, Phys. Rev. Lett. **64**, 821 (1990); A. Prasad, L. D. Iasemmidis, S. Sabesan, and K. Tsakalis, Pramana, J. Phys. **64**, 513 (2005).

[7] H. Fujisaka and T. Yamada, Prog. Theor. Phys. **69**, 32 (1983).

[8] A. S. Pikovsky, Z. Phys. B **55**, 149 (1984).

[9] M. de Sousa Vieira, A. J. Lichtenberg, and M. A. Lieberman, Int. J. Bifurcation Chaos Appl. Sci. Eng. **1**, 691 (1991).
[10] N. F. Rulkov, M. M. Sushchik, L. S. Tsimring, and H. D. I. Abarbanel, Phys. Rev. E **51**, 980 (1995); H. D. I. Abarbanel, N. F. Rulkov, and M. M. Sushchik, *ibid.* **53**, 4528 (1996).
[11] M. G. Rosenblum, A. S. Pikovsky, and J. Kurths, Phys. Rev. Lett. **76**, 1804 (1996); **78**, 4193 (1997).
[12] Y. Kuramoto, *Chemical Oscillations, Waves, and Turbulence* (Springer, New York, 1984); R. E. Mirollo and S. H. Strogatz, SIAM J. Appl. Math. **50**, 1645 (1990); N. Kopell, G. B. Ermentrout, M. A. Whittington, and R. D. Traub, Proc. Natl. Acad. Sci. U.S.A. **97**, 1867 (2000); T. J. Lewis and J. Rinzel, J. Comput. Neurosci. **14**, 283 (2003); E. M. Izhikevich, *Dynamical Systems in Neuroscience: The Geometry of Excitability and Bursting* (MIT Press, Cambridge, MA, 2007); A. Sherman, J. Rinzel, and J. Keizer, Biophys. J. **54**, 411 (1988); M. G. Pedersen, R. Bertram, and A. Sherman, *ibid.* **89**, 107 (2005).
[13] J. F. Heagy and S. M. Hammel, Physica D **70**, 140 (1994).
[14] K. Kaneko, Prog. Theor. Phys. **71**, 1112 (1984); T. Nishikawa and K. Kaneko, Phys. Rev. E **54**, 6114 (1996).
[15] A. Prasad, V. Mehra, and R. Ramaswamy, Phys. Rev. Lett. **79**, 4127 (1997).
[16] A. Witt, U. Feudel, and A. S. Pikovsky, Physica D **109**, 180 (1997).
[17] A. S. Pikovsky, M. A. Zaks, U. Feudel, and J. Kurths, Phys. Rev. E **52**, 285 (1995).
[18] A. Prasad, A. Nandi, and R. Ramaswamy, Int. J. Bifurcat. Chaos **17**, 3397 (2007).
[19] A. S. Pikovsky and U. Feudel, J. Phys. A **27**, 5209 (1994).
[20] T. Yalçinkaya and Y.-C. Lai, Phys. Rev. Lett. **77**, 5039 (1996); Phys. Rev. E **56**, 1623 (1997).
[21] A. S. Pikovsky and U. Feudel, Chaos **5**, 253 (1995).
[22] M. G. Rosenblum, A. S. Pikovsky, and J. Kurths, IEEE Trans. Circ. Syst. **44**, 874 (1997).
[23] A. S. Pikovsky, M. G. Rosenblum, and J. Kurths, Europhys. Lett. **34**, 165 (1996).
[24] A. Goryachev and R. Kapral, Phys. Rev. Lett. **76**, 1619 (1996).
[25] E.-H. Park, M. A. Zaks, and J. Kurths, Phys. Rev. E **60**, 6627 (1999).
[26] M. D. Shrimali, A. Prasad, R. Ramaswamy, and U. Feudel, Phys. Rev. E **72**, 036215 (2005).
[27] R. Ramaswamy, Phys. Rev. E **56**, 7294 (1997).
[28] M. Agrawal (unpublished).
[29] C. Schäfer, M. G. Rosenblum, J. Kurths, and H.-H. Abel, Nature (London) **392**, 239 (1998); C. Schäfer, M. G. Rosenblum, H.-H. Abel, and J. Kurths, Phys. Rev. E **60**, 857 (1999).
[30] A. J. Mandell and K. A. Selz, J. Stat. Phys. **70**, 355 (1993).